Supporting Information

Polyimide with enhanced π stacking for efficient visible-light-driven photocatalysis

Kelian Zhang,[a] Hanmei Li,[a] Haixian Shi[a] and Wei Hong[*a]*

a. Key Laboratory for Polymeric Composite and Functional Materials of Ministry of Education, Guangdong Engineering Technology Research Center for High-performance Organic and Polymer Photoelectric Functional Films, School of Chemistry, Sun Yat-sen University, Guangzhou 510275, P. R. China.
*E-mail: hongwei9@mail.sysu.edu.cn.

Contents Page

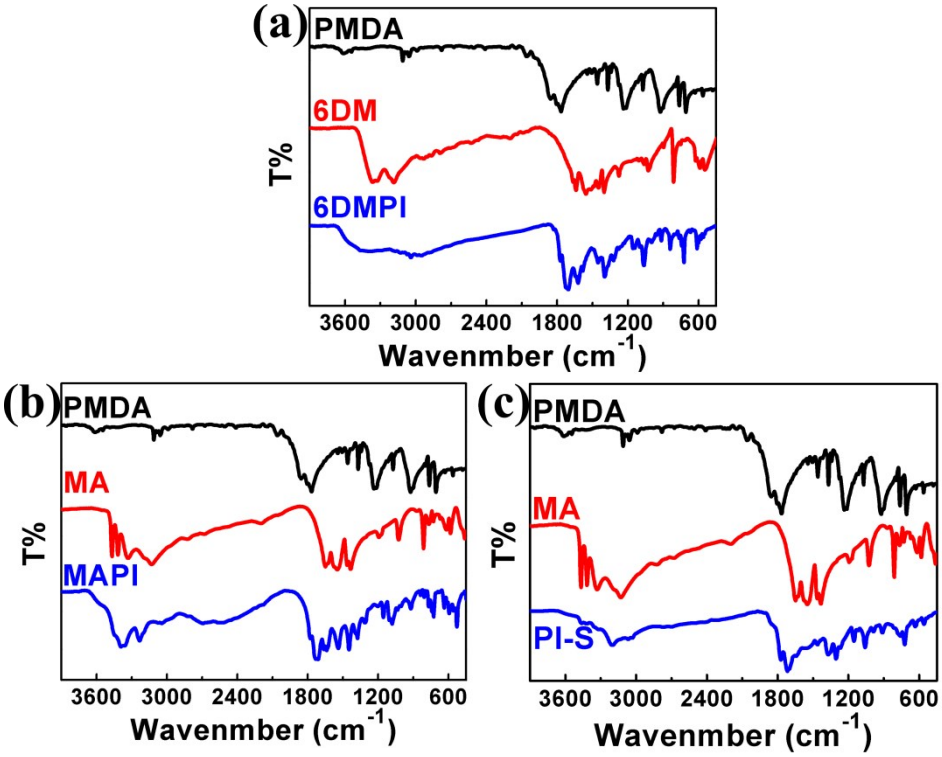

Figure S1 FT-IR spectra of (a) 6DMPI, (b) MAPI and (c) PI-S

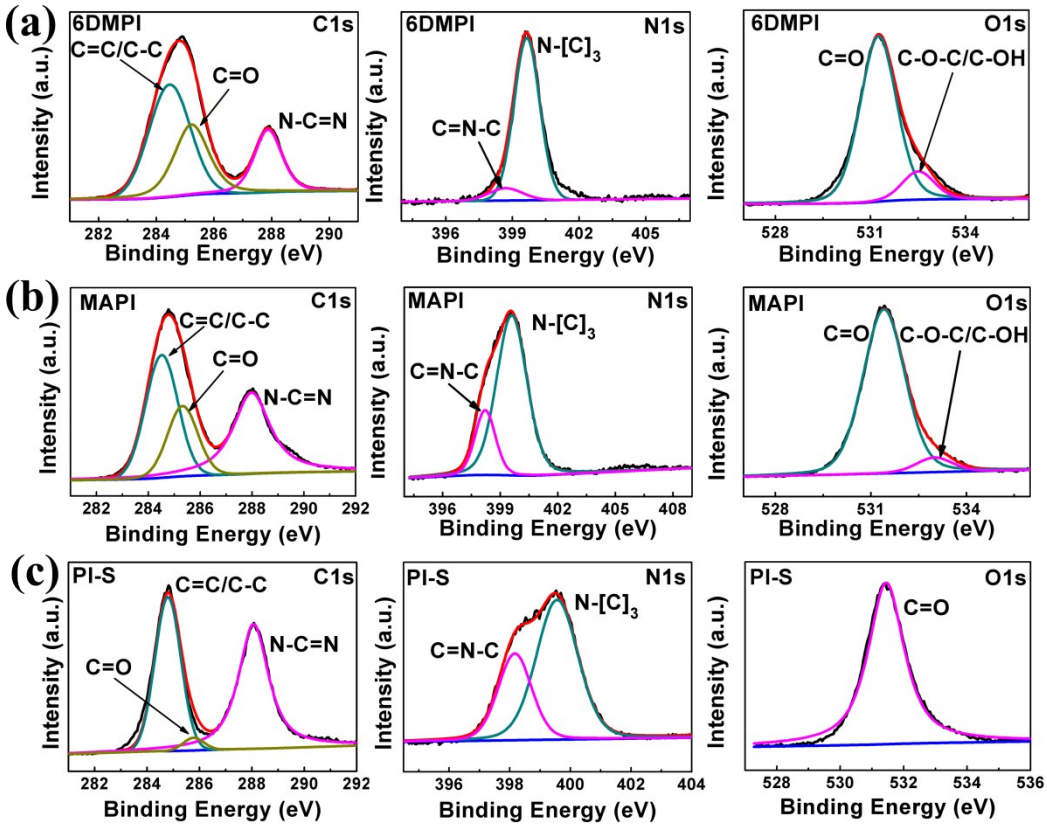

Figure S2 XPS spectra of (a) 6DMPI, (b) MAPI, (c) PI-S.

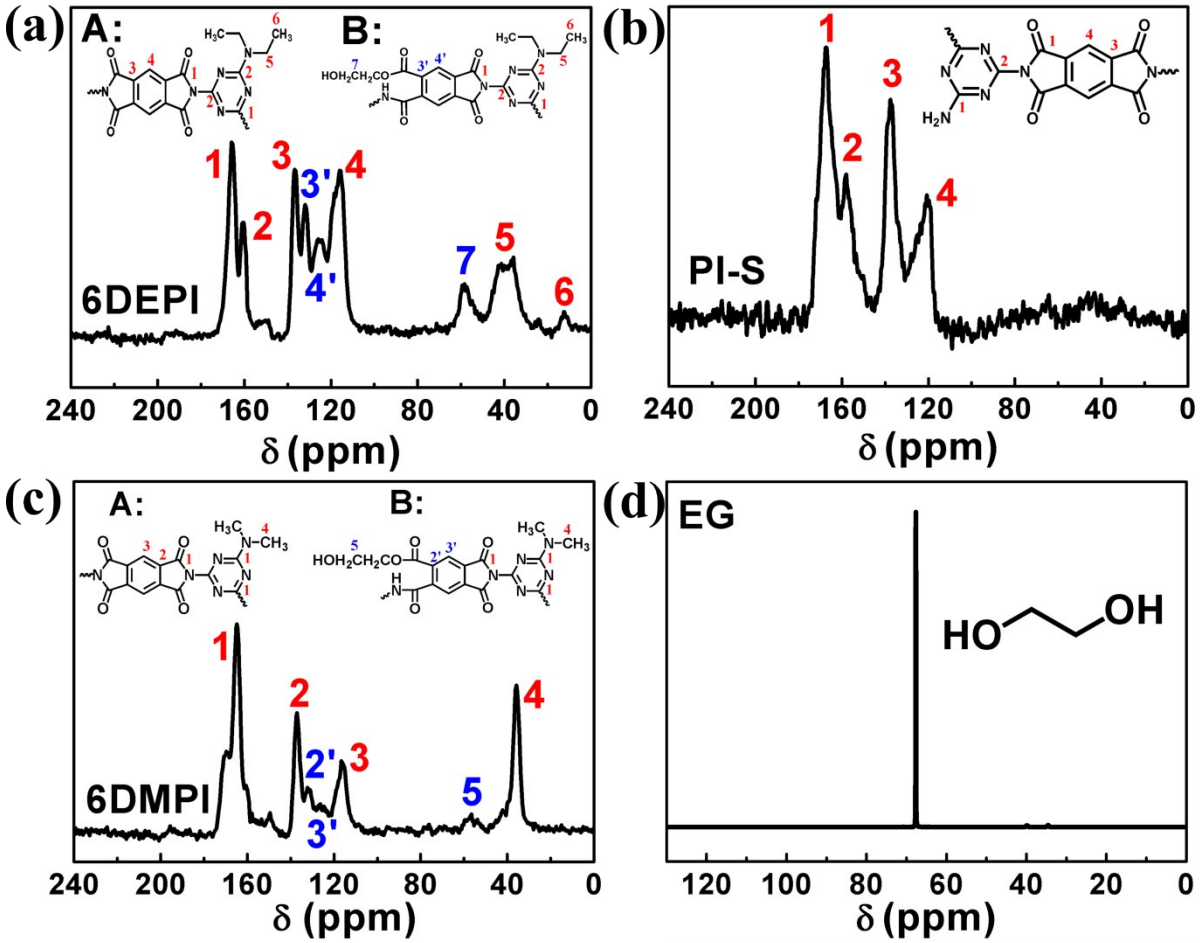

Figure S3 (a), (b), (c) Solid-state ^{13}C NMR spectra of 6DEPI, PI-S and 6DMPI, respectively. (d) ^{13}C NMR spectra of glycol in DMF.

Table S1 Elemental analysis result of atomic contents of the PI-based photocatalysts and g-C_3N_4.

Sample	C%	N%	H%	C/N ratio	C/H ratio
6DEPI	56.98	12.94	4.02	4.40	14.17
6DMPI	54.70	12.93	3.65	4.23	14.99
MAPI	42.63	32.48	3.26	1.31	13.08
PI-S	48.97	23.57	2.14	2.08	22.94
g-C_3N_4	36.36	58.85	4.79	0.62	7.59

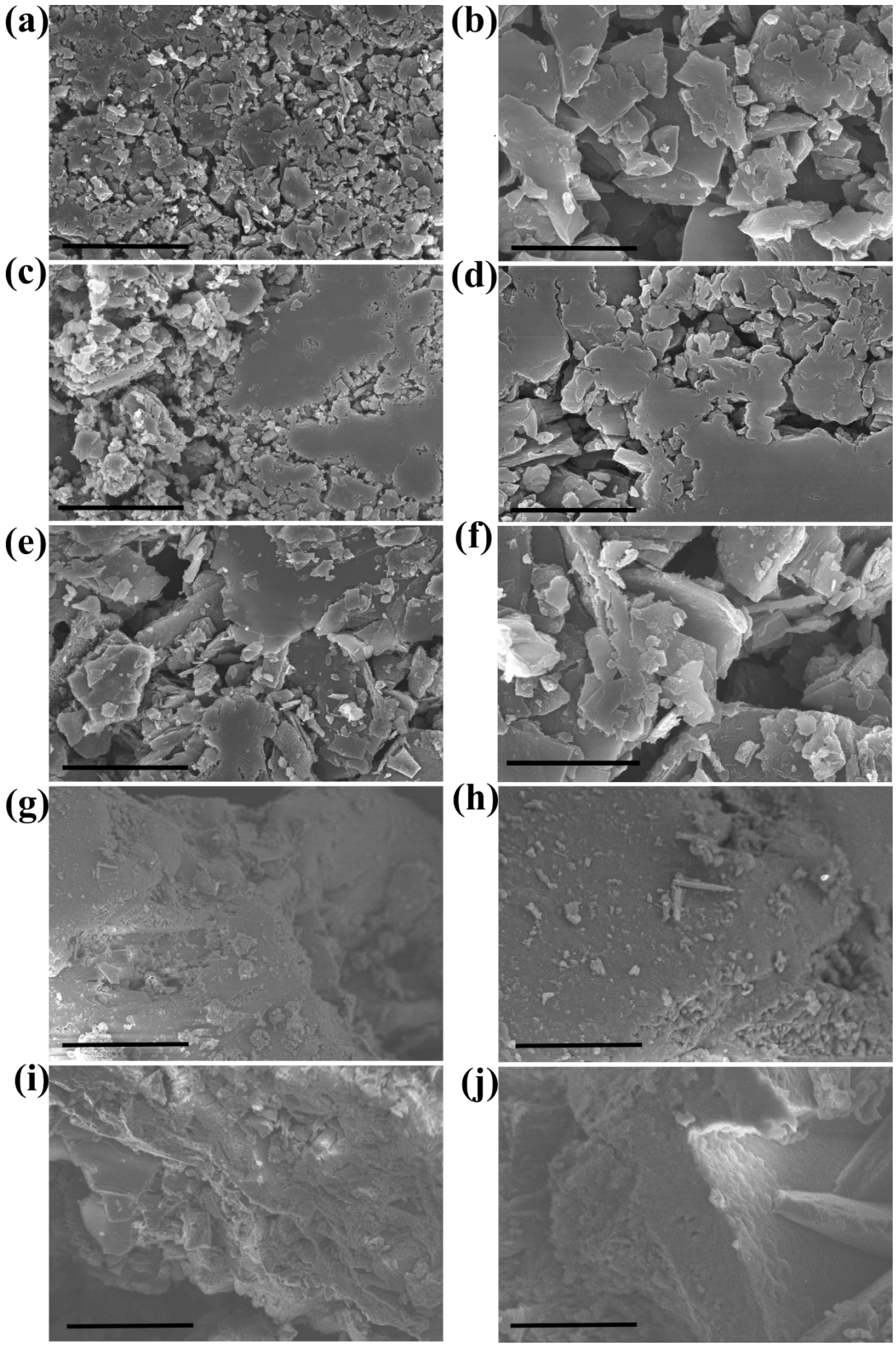

Figure S4 (a), (b) SEM images of 6DEPI, scale bar: 20 μm, 5 μm, respectively. (c), (d) SEM images of 6DMPI, scale bar: 20 μm, 5 μm, respectively. (e), (f) SEM images of MAPI, scale bar: 20 μm, 5 μm, respectively. (g), (h) SEM images of PI-S, scale bar: 20 μm, 5 μm, respectively. (i), (j) SEM images of g-C_3N_4, scale bar: 20 μm, 5 μm, respectively.

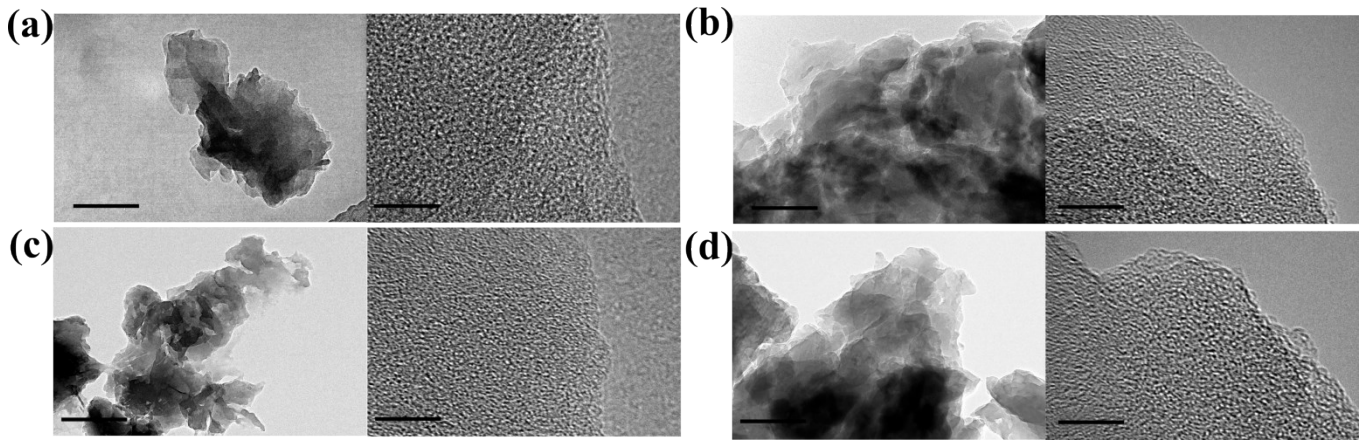

Figure S5 (a) TEM images of 6DMPI, scale bar: 100 nm and 5 nm, respectively. (b) TEM images of MAPI, scale bar: 100 nm and 5 nm, respectively.(c) TEM images of PI-S, scale bar: 100 nm and 5 nm, respectively.(d) TEM images of g-C_3N_4, scale bar: 100 nm and 5 nm, respectively.

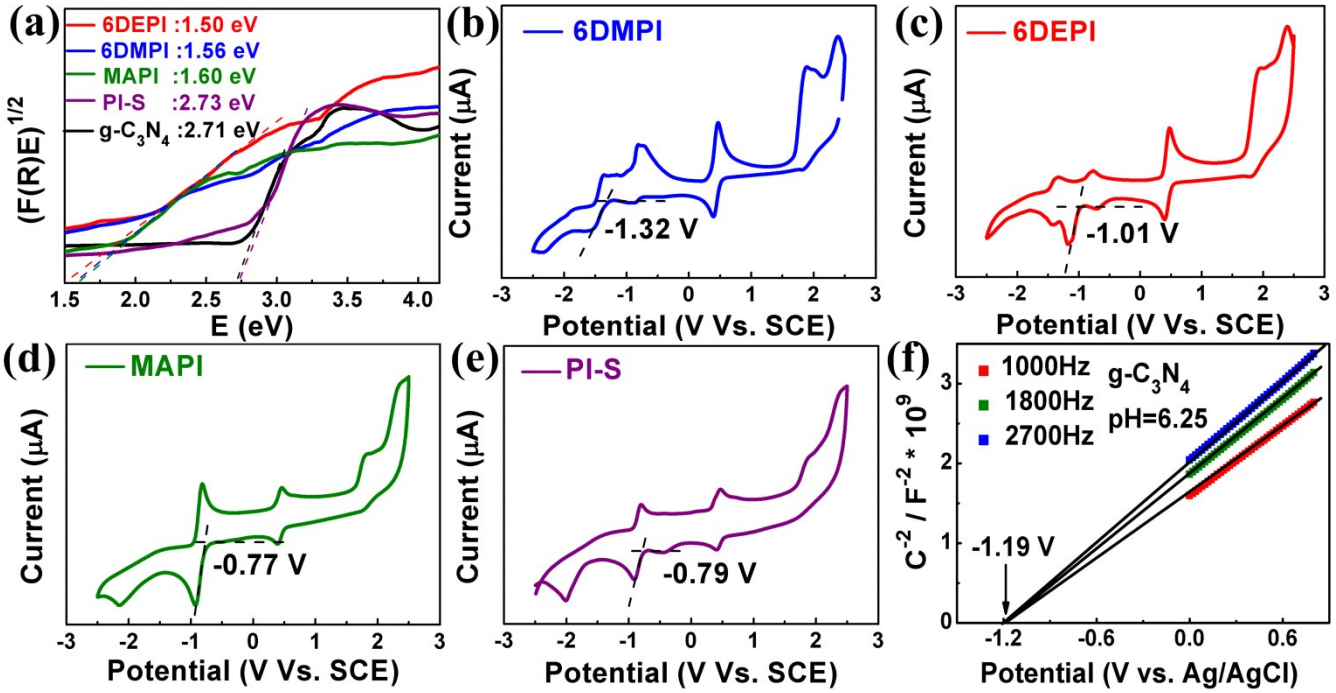

Figure S6 (a) Tauc plots and the apparent band gaps of pristine g-C_3N_4, PI-S, MAPI, 6DMPI and 6DEPI, based on the Kubelka-Munk of rmula according to the results of UV-vis DRS spectrum. (b), (c), (d) and (e) CVs of 6DMPI, 6DEPI, MAPI and PI-S, respectively. (The weak anodic peak appears at 0.46 V and the coresponding cathodic peak at 0.39 V are the oxidation and reduction potential of Fc/Fc^+.) (f) Mott-Schottky plots of g-C_3N_4. The E_{CB} values of g-C_3N_4 were estimated by $E_{CB}\,(vs.NHE) = E_{red}\,(vs.\ Ag/AgCl\,) + 0.197\,V$, the E_{VB}=Eg-E_{CB}. The E_{CB} values of 6DEPI, 6DEPI, MAPI and PI-S was estimated by $E_{CB}\,(vs.\,NHE) = E_{red}\,(vs.\ SCE) + 0.24\,V$.

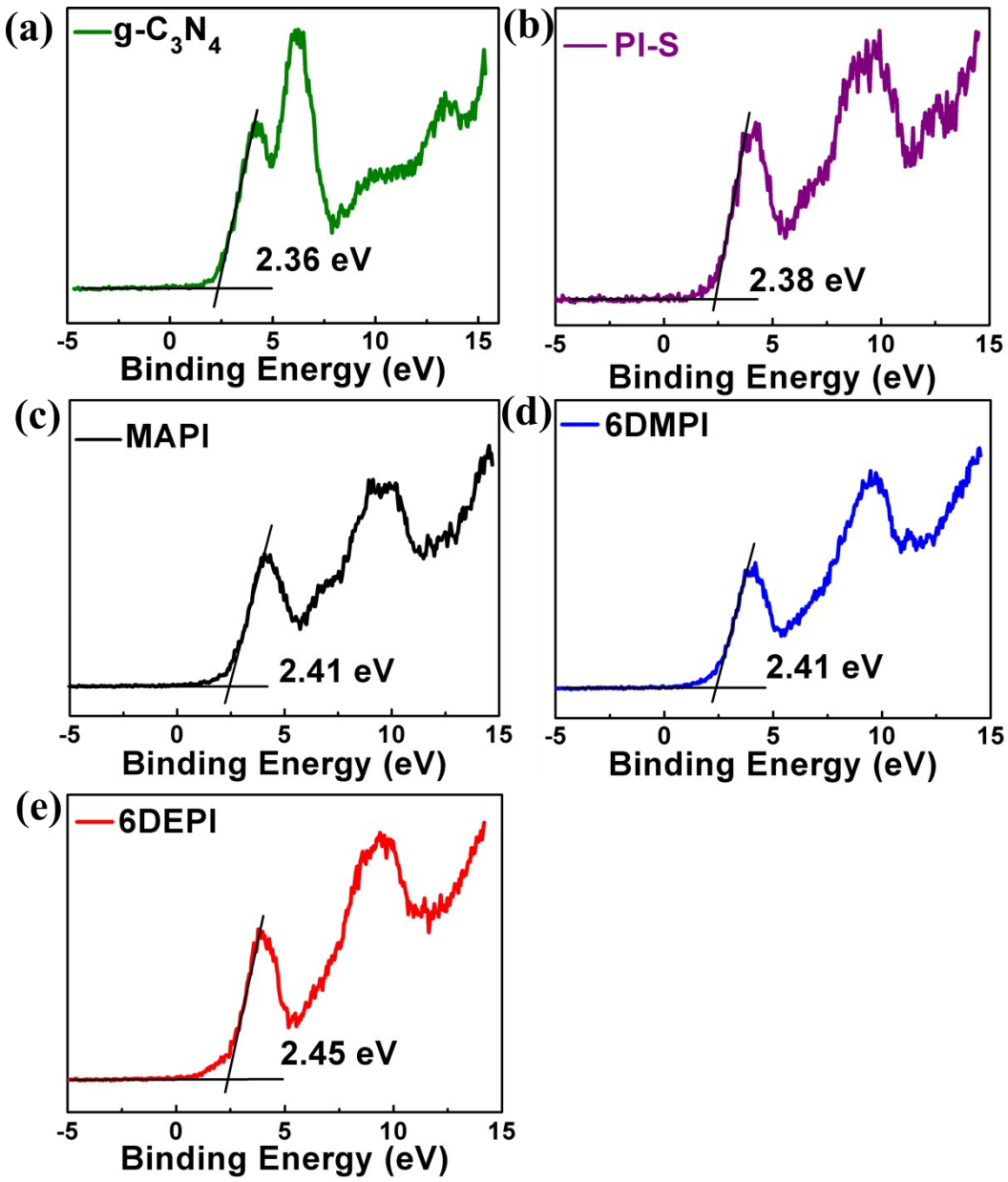

Figure S7 (a), (b), (c),(d) and (e) VB-XPS spectrum of pristine g-C_3N_4,PI-S, MAPI, 6DMPI and 6DEPI, respectively.

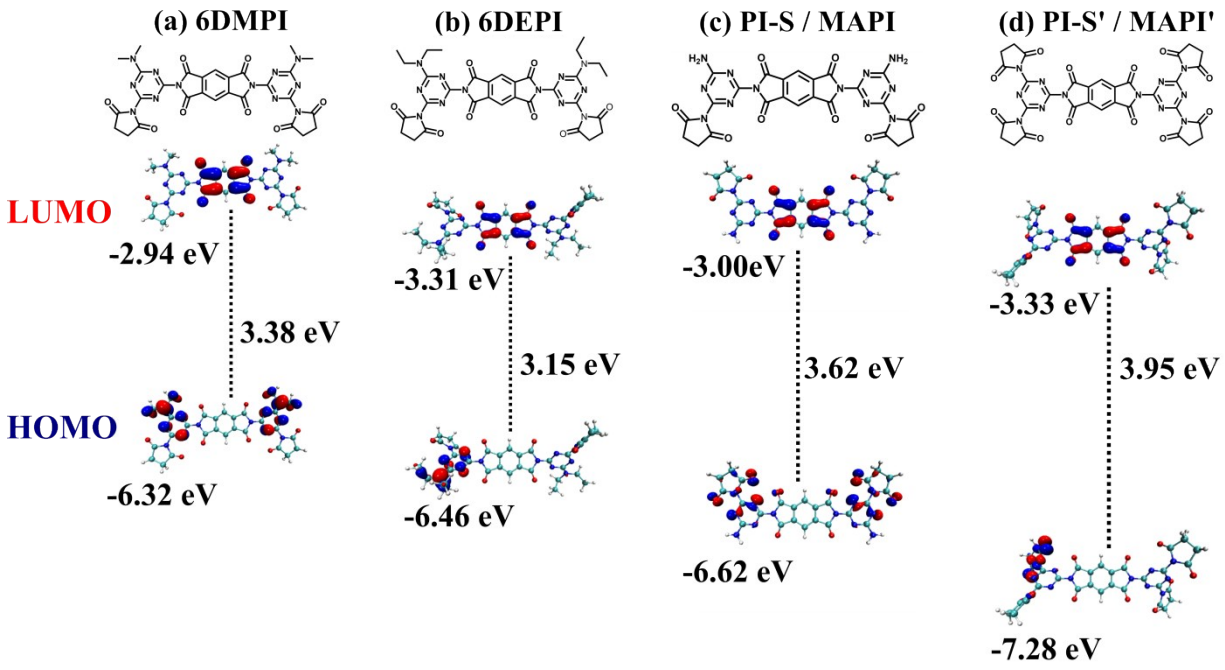

Figure S8 HOMO and LUMO orbitals of the geometry-optimized PI model, (a) 6DMPI, (b) 6DEPI, (c) PI-S/MAPI and (d) PI-S′/MAPI′ (crosslinked), respectively.

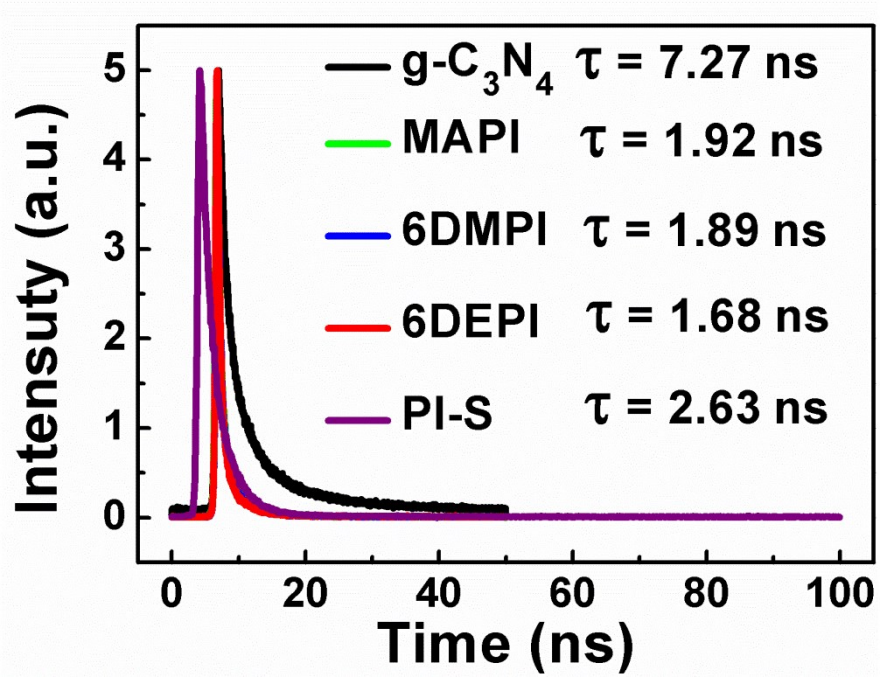

Figure S9 Time-resolved PL spectra of g-C_3N_4, PI-S, MAPI, 6DMPI and 6DEPI, respectively, monitored at 470, 550, 580 and 580 nm, respectively, under 406 nm excitation at 298 K.

Table S2 The measured lifetime of g-C_3N_4, MAPI, 6DMPI and 6DEPI, respectively. The average lifetime was calculated using equation: $\tau = (A_1\tau_1 + A_2\tau_2 + A_3\tau_3)$

Sample	τ_1 [ns]	A_1 [%]	τ_2 [ns]	A_2 [%]	τ_3 [ns]	A_3 [%]
g-C_3N_4	0.96	15.18	3.60	45.04	14.00	39.77
PI-S	1.58	50.15	3.69	49.85		
MAPI	0.41	36.52	2.02	46.27	4.87	17.21
6DMPI	0.51	52.51	3.07	47.49		
6DEPI	0.48	52.09	2.99	47.91		

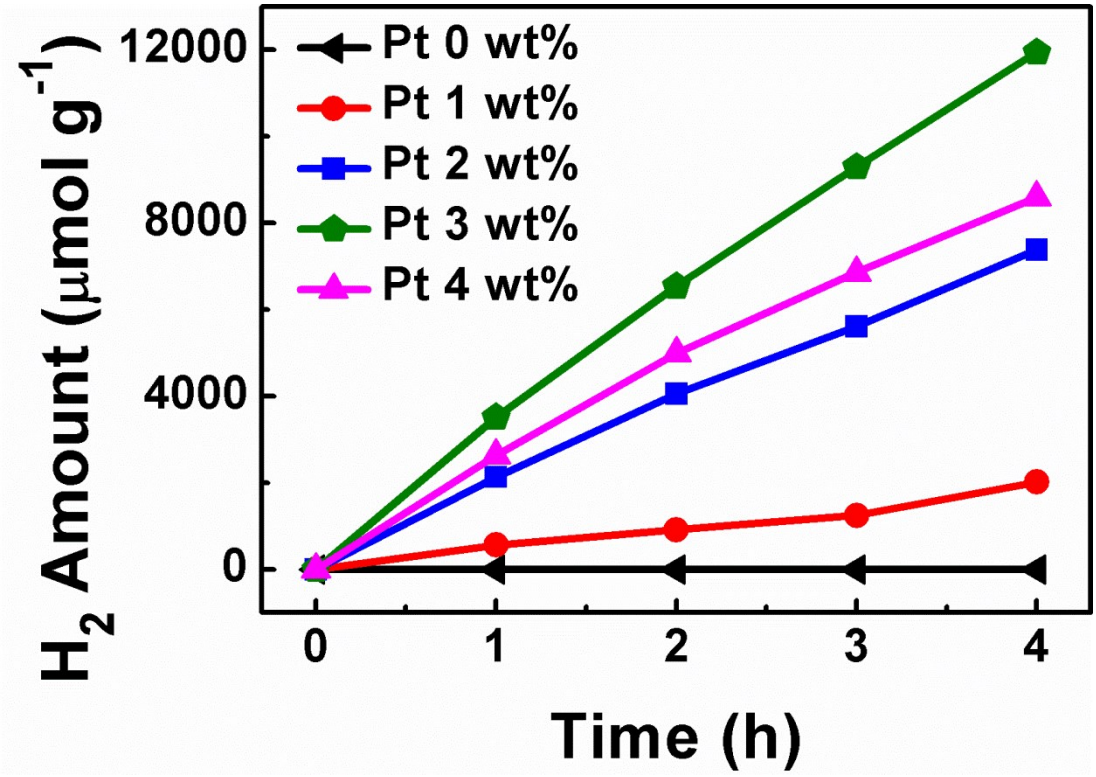

Figure S10 The HER of 6DEPI with different mass ratios of Pt.

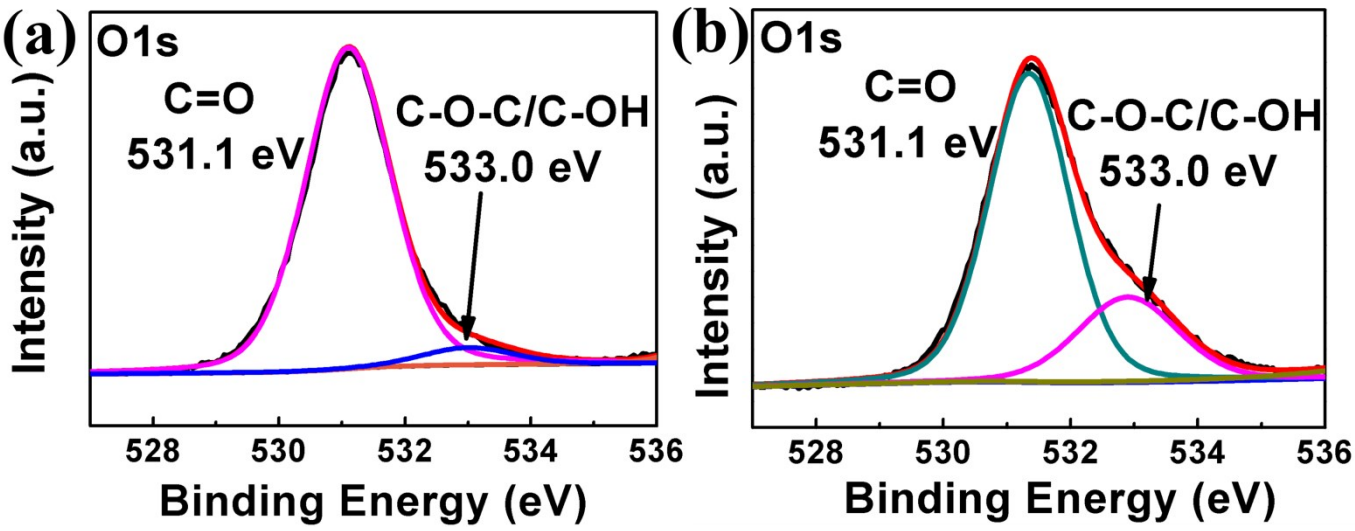

Figure S11 (a) The O1s XPS spectra of 6DEPI before hydrogen evolution tests, (b) The O1s XPS spectra of 6DEPI after hydrogen evolution tests.

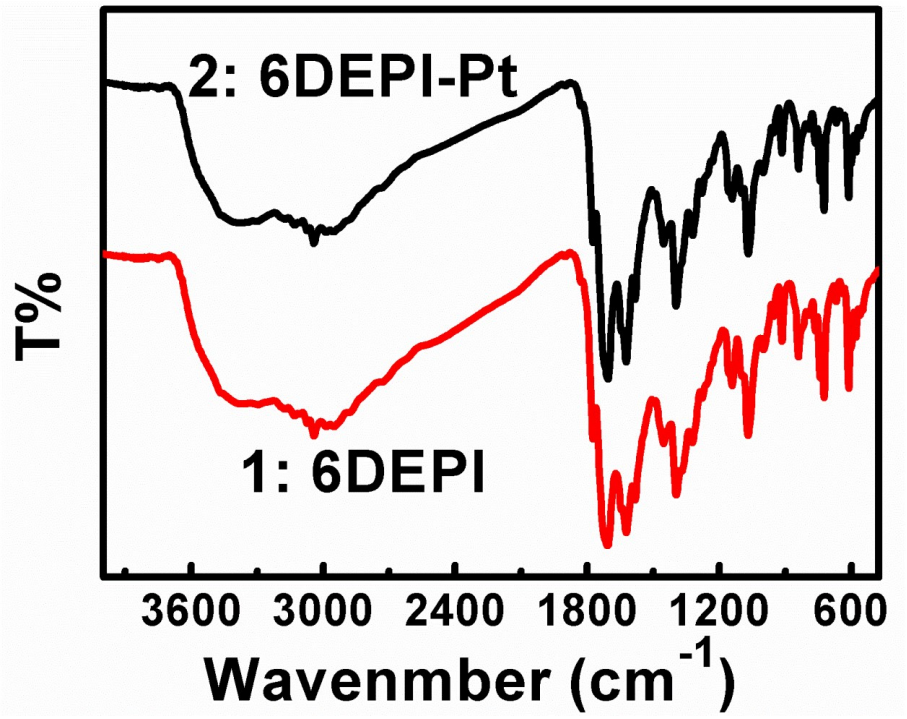

Figure S12 1, FT-IR spectra of 6DEPI before HER reactions. 2, FT-IR spectra of 6DEPI after HER reactions, named as 6DEPI-Pt. The mass ratios of Pt was 3 wt%.

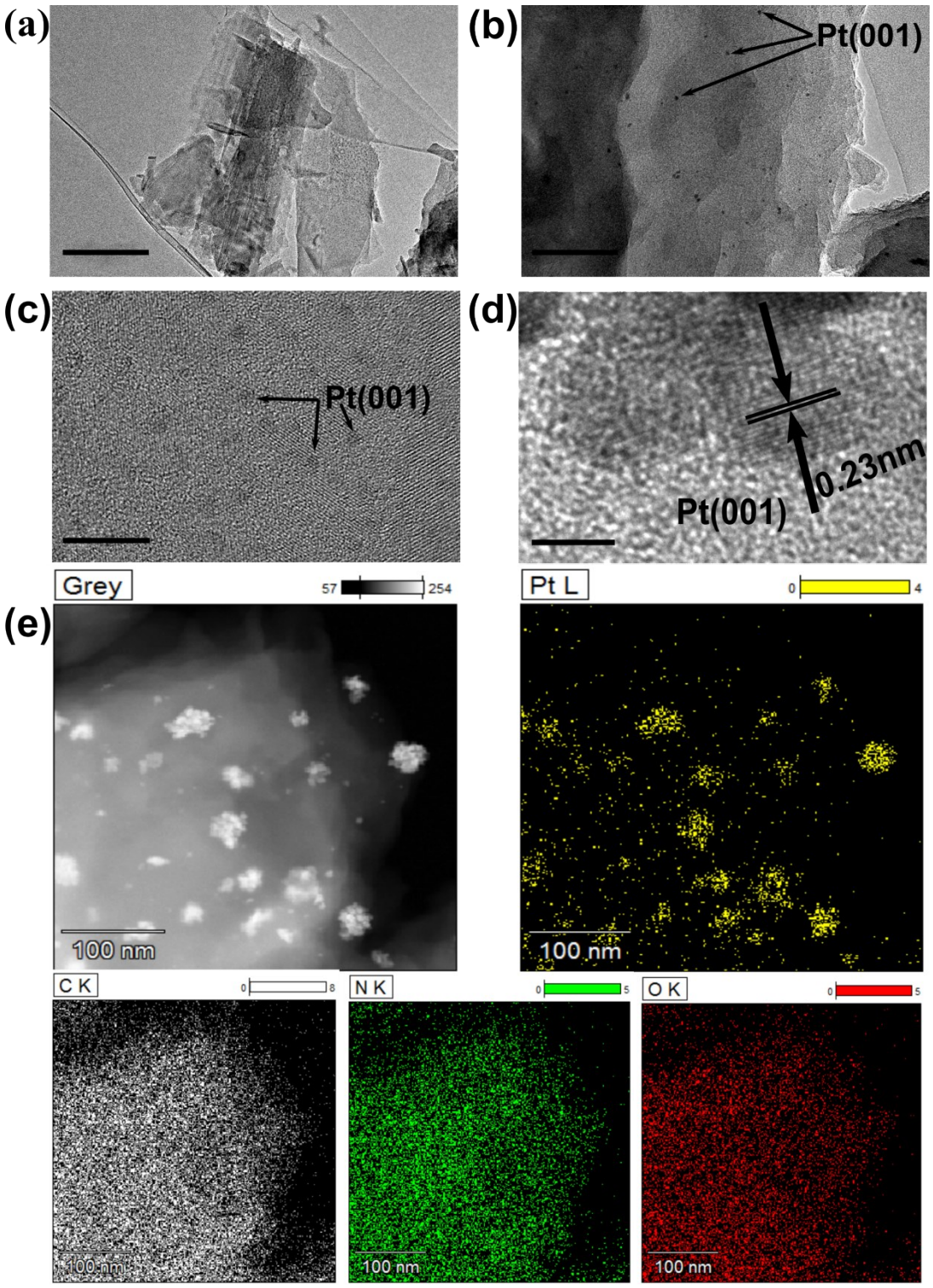

Figure S13 TEM images of 6DEPI-Pt. (a) scale bar: 100 nm, (b) scale bar: 50 nm, (c) scale bar: 5 nm, (d) scale bar: 2 nm. (e) EDS images of 6DEPI-Pt. The mass ratios of Pt was 3 wt%.

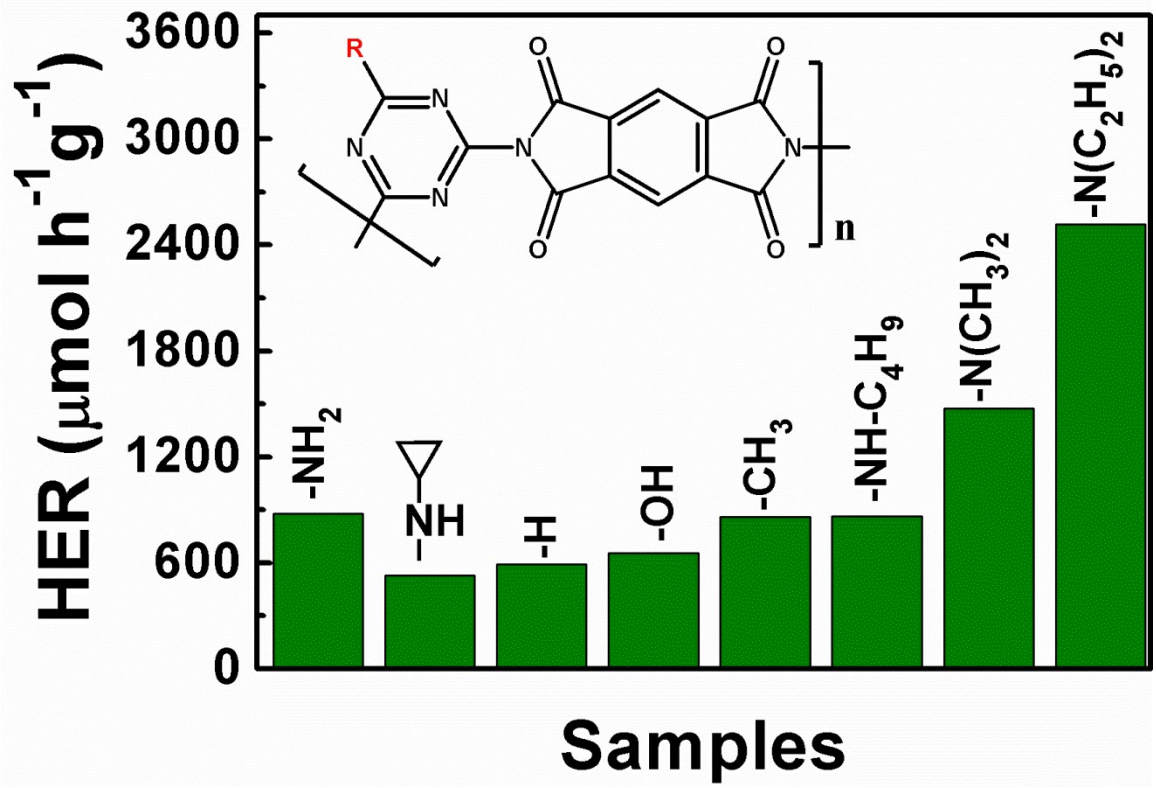

Figure S14 HER of different PI-based photocatalysts.

Table S3 Hydrogen evolution rate (HER) comparison of PI-based photocatalysts.

Reference	photocatalysts	HER (μmol h^{-1} g^{-1})	Regulation Method	Experimental Conditions (λ>420 nm)
This work	6DEPI	2516 (initial) 3812 (for the 2nd run)	Linear PI through solvothermal synthesis	TEOA as a sacrificial reagent and 3 wt% Pt as a cocatalyst
S1	PI	35	direct heating the mixture of Melem and PMDA	methanol as a sacrificial reagent and 1 wt% Pt as a cocatalyst

S2	PI	103	direct heating the mixture of Melem and PMDA	methanol as a sacrificial reagent and 1 wt% Pt as a cocatalyst
S3	PI-1	65	direct heating the mixture of Melem and PMDA	methanol as a sacrificial reagent and 1 wt% Pt as a cocatalyst
S3	PI-2	6	direct heating the mixture of Melem and BPDA	methanol as a sacrificial reagent and 1 wt% Pt as a cocatalyst
S3	PI-3	6.5	direct heating the mixture of Melem and NTDA	methanol as a sacrificial reagent and 1 wt% Pt as a cocatalyst
S4	PI-325	76	direct heating the mixture of Melem and PMDA	methanol as a sacrificial reagent and 1 wt% Pt as a cocatalyst
S5	PI-SM-180	1640	Melem and PDMA through solvothermal synthesis	methanol as a sacrificial reagent and 3 wt% Pt as a cocatalyst (λ>300 nm)
S6	PI-DMF	120	Melem and PDMA through solvothermal synthesis	methanol as a sacrificial reagent and 3 wt% Pt as a cocatalyst (λ>300 nm)
S7	MPI_7	184	Melem and PDMA through MW-assisted heating method	TEOA as a sacrificial reagent and 0.5 wt% Pt as a cocatalyst

S8	PI/Ag aerogel photocatalysts	166.1	ODA and PBDA through sol–gel method	methanol as a sacrificial reagent
S9	MQDs/PI	630	MoS_2 quantum dots heterojunction through immersion-hydrothermal method	methanol as a sacrificial reagent
S10	CdS/PI	613	CdS/PI heterojunction through solvothermal method	methanol as a sacrificial reagent

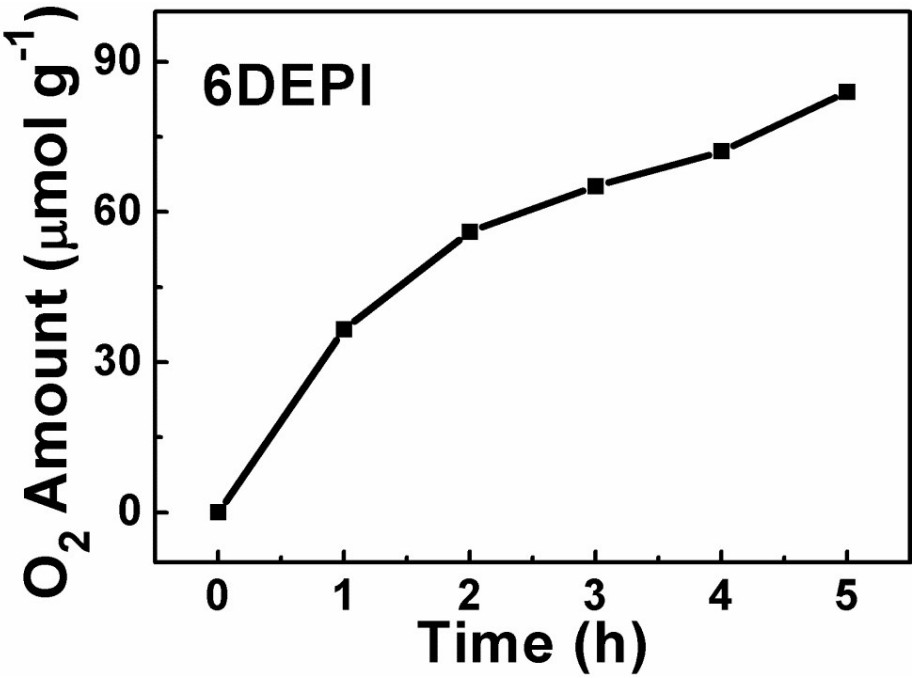

Figure S15 The photocatalytic oxygen evolution with 6DEPI

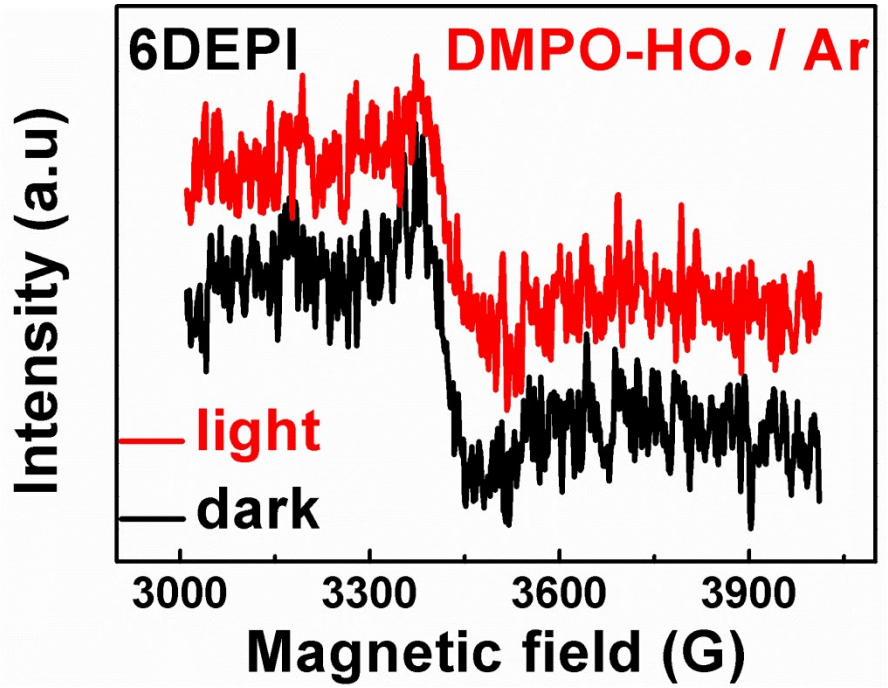

Figure S16 Under Ar atmosphere, DMPO spin-trapping ESR spectra for DMPO-HO• produced by 6DEPI in water with visible light irradiation time of 6 min. The result indicated that no HO• was generated under visible light irradiation.

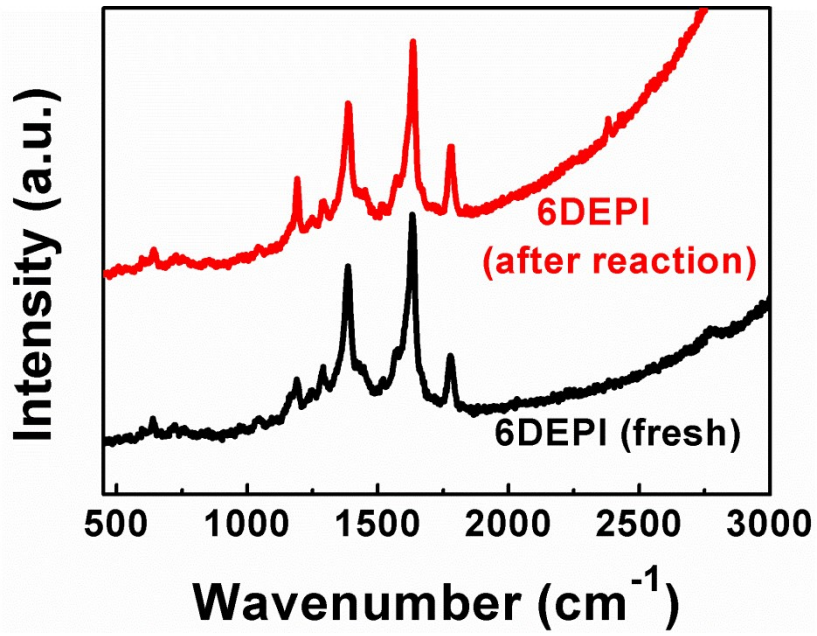

Figure S17 The Raman spectra of 6DEPI before and after H_2O_2 evolution.

References of supporting Information :

1. S. Chu, Y. Wang, Y. Guo, P. Zhou, H. Yu, L. Luo, F. Kong and Z. Zou, *J. Mater. Chem.*, 2012, **22**.

2. S. Chu, Y. Wang, Y. Guo, J. Feng, C. Wang, W. Luo, X. Fan and Z. Zou, *ACS Catal*., 2013, **3**, 912-919.
3. S. Chu, C. Wang, J. Feng, Y. Wang and Z. Zou, *Int. J. Hydrogen Energy*, 2014, **39**, 13519-13526.
4. S. Chu, Y. Wang, C. Wang, J. Yang and Z. Zou, *Int. J. Hydrogen Energy*, 2013, **38**, 10768-10772.
5. J. Zhou, Y. Lei, C. Ma, W. Lv, N. Li, Y. Wang, H. Xu and Z. Zou, *Chem. Commun*., 2017, **53**, 10536-10539.
6. J. Zhou, Y. Wang, X. Hao, C. Ma, Y. Wang and Z. Zou, *J. Phys. Chem. C*, 2018, **122**, 1037-1043.
7. L. Lin, P. Ye, C. Cao, Q. Jin, G.-S. Xu, Y.-H. Shen and Y.-P. Yuan, *J. Mater. Chem. A,* 2015, **3**, 10205-10208.
8. X. Zhao, X. Yi, X. Wang, W. Chu, S. Guo, J. Zhang, B. Liu and X. Liu, Appl. Surf. Sci., 2020, **502**, 144187.
9. C. Ma, H. Zhu, J. Zhou, Z. Cui, T. Liu, Y. Wang, Y. Wang and Z. Zou, *Dalton Transactions*, 2017, **46**, 3877-3886.
10. Y. Hu, X. Hao, Z. Cui, J. Zhou, S. Chu, Y. Wang and Z. Zou, *Appl. Catal., B*, 2020, **260**, 118131.